The Journal of Experimental Biology 216, 4462-4472

doi:10.1242/jeb.094912

RESEARCH ARTICLE

Phylogeny and effects of anoxia on hyperpolarization-activated cyclic nucleotide-gated channel gene expression in the heart of a primitive chordate, the Pacific hagfish (*Eptatretus stoutii*)

Christopher M. Wilson[1,*], Jonathan A. W. Stecyk[2], Christine S. Couturier[3], Göran E. Nilsson[3] and Anthony P. Farrell[1,4]

[1]Department of Zoology, University of British Columbia, Vancouver, BC, Canada, V6T 1Z4, [2]Department of Biological Sciences, University of Alaska Anchorage, Anchorage, AK 99508, USA, [3]Programme for Physiology and Neurobiology, Department of Biosciences, University of Oslo, PO Box 1066, N-0316, Oslo, Norway and [4]Faculty of Land Food Systems, University of British Columbia, Vancouver, BC, Canada, V6T 1Z4

*Author for correspondence (chris7_77@hotmail.com)

SUMMARY

The aneural heart of the Pacific hagfish, *Eptatretus stoutii*, varies heart rate fourfold during recovery from anoxia. Hyperpolarization-activated cyclic nucleotide-gated (HCN) channels, which play an important role in establishing the pacemaker rate of vertebrate hearts, were postulated to be present in this ancestral vertebrate heart, and it was also theorized that changes in hagfish heart rate with oxygen availability involved altered HCN expression. Partial gene cloning revealed six HCN isoforms in the hagfish heart. Hagfish representatives of HCN2, HCN3 and HCN4 were discovered, with HCN2 and HCN3 existing as isoforms designated as HCN2a, HCN2b, HCN3a, two paralogs of HCN3b, and HCN3c. Phylogenetic analysis revealed HCN3b and HCN3c to be ancestral, followed by HCN3a, HCN4 and HCN2. Moreover, HCN3a expression was dominant in both the atrial and ventricular chambers, suggesting that the HCN4 dominance in adult mammalian hearts appeared after hagfish divergence. HCN expression was higher in the atrium than in the ventricle, as might be expected given that atrial beating rate is known to be faster than the ventricular rate. In addition, mRNA expression under normoxic conditions was compared with that following 24 h of anoxia, and either a 2-h or 36-h recovery in normoxic water. In the ventricle, anoxia decreased HCN3a but not HCN4 expression. In contrast, atrial HCN3a expression significantly increased following 2 h of recovery, before returning to control levels following 36 h of recovery, possibly contributing to heart rate changes previously observed under these conditions.

Key words: fish, cardiac control, pacemaker, real-time reverse transcriptase PCR, anoxia, HCN channel, phylogeny.

Received 31 July 2013; Accepted 19 August 2013

INTRODUCTION

The regular vertebrate heartbeat requires no external input and is initiated by specialized pacemaker cells located in the sinoatrial node (DiFrancesco, 1993). These pacemaker cells have a Ca^{2+}-mediated upstroke to the action potential rather than the Na^{+}-mediated one that characterizes contractile cardiac myocytes. In addition, pacemaker cells have a slowly depolarizing membrane potential, known as the pacemaker potential, rather than the stable membrane potential present between action potentials characteristic of the working myocardium (Brown and DiFrancesco, 1980; Doerr et al., 1989; Baker et al., 1997; DiFrancesco, 2010). In mammals, the pacemaker potential is a result of inward cation currents. These comprise a mixed K^{+} and Na^{+} current (I_f) flowing through hyperpolarization-activated cyclic nucleotide-gated (HCN) protein channels in the cell membrane, and an inward sodium/calcium exchange current (I_{NCX}) activated by rhythmic cycling of Ca^{2+} through the sarcoplasmic reticulum (DiFrancesco and Ojeda, 1980; Yanagihara and Irisawa, 1980; Dobrzynski et al., 2007; Maltsev and Lakatta, 2008; Monfredi et al., 2013). The magnitude of these inward currents directly affects the slope of the pacemaker potential, which, in turn, sets heart rate by determining the time taken to reach the threshold voltage needed to open the Ca^{2+} channel (DiFrancesco and Tortora, 1991; Wainger et al., 2001).

The ancestral hagfishes are believed to have diverged from the vertebrate lineage over 500 million years ago and prior to the genome duplications postulated for the vertebrate lineage (Ota and Kuratani, 2007). Despite their evolutionary importance, knowledge on cardiac pacemaker mechanisms in hagfishes is very limited (Farrell, 2007; Wilson and Farrell, 2013). The hagfish heart is unique by being the only vertebrate-type, myogenic heart that is anatomically aneural. However, despite aneural control, heart rate can vary fourfold during recovery from prolonged anoxia (Greene, 1902; Augustinsson et al., 1956; Jensen, 1961; Hirsch et al., 1964; Jensen, 1965; Farrell, 2007; Cox et al., 2010). Recent work suggests that the sarcoplasmic reticulum plays a very minor, if any, role in hagfish cardiac pacemaking, whereas the central importance of HCN channels in setting the intrinsic heart rate is implied by the finding that the HCN channel antagonist zatebradine almost stops the heartbeat (Wilson and Farrell, 2013).

HCN channels are closely related to the ether-à-go-go and cyclic nucleotide-gated K^{+} channels. It is thought that HCN channels consist of four protein subunits, each with six transmembrane segments, a voltage sensor, an ion-conducting pore and an

evolutionarily conserved cyclic nucleotide-binding domain (CNBD) (Doyle et al., 1998; Ishii et al., 1999; Jiang et al., 2003). CNBD inhibition of I_f is inversely related to the concentration of cAMP (Wang et al., 2001; Biel et al., 2002). Neural and humoral stimulation can modulate adenylate cyclase activity, changing cytosolic cAMP concentration, which then alters the inhibition imposed by the CNBD (Brown et al., 1979a; Brown et al., 1979b; Brown and DiFrancesco, 1980; DiFrancesco, 1985; DiFrancesco, 2010). Furthermore, in mammals, the relative expression of the four HCN isoforms (HCNs 1–4), each of which has different electrophysiological properties, can vary among tissues. For example, expression of HCN4 is dominant in adult mammalian atria, whereas HCN2 is dominant in the ventricle (Moosmang et al., 2001; Qu et al., 2002; Shi et al., 1999).

The genes encoding the four mammalian HCN isoforms are highly conserved among other vertebrate hearts. A large-scale phylogenetic study (Jackson et al., 2007) suggested that the four HCN isoforms arose from duplications of a single HCN ancestral gene most similar to HCN3, with some teleost fishes having extra isoforms that likely arose from lineage-specific gene or genome duplications. Outside the vertebrates, in *Ciona*, lineage-specific duplications of the ancestral gene have resulted in three *Ciona*-specific HCN isoforms (Jackson et al., 2007). Surprisingly, nothing is known about the quantity or regulation of HCN in hagfishes, which occupy the basal position in vertebrate evolution and possess a vertebrate-type, myogenic heart with valved chambers, unlike *Ciona*. Here, we postulate that modulation of HCN channels is central to the control of hagfish heart rate, in that the decrease in heart rate seen by Cox et al. (Cox et al., 2010) in anoxia results from a decrease in HCN channel expression, and the following increase in heart rate upon reoxygenation is coupled with an increase in HCN channel expression.

To test this hypothesis, we partially cloned hagfish cardiac HCN isoforms from atria and ventricles and compared them with known vertebrate isoforms to establish where the hagfish fits within the chordate phylogeny. In addition, real-time reverse transcriptase PCR (RT-PCR) was utilized to examine the mRNA expression of HCN isoforms in the hagfish heart before, during and after an anoxic challenge to test for plasticity in the expression of HCN. Both cardiac chambers were examined because pacemaker activity has been recorded from multiple areas of the atrium and ventricle in hagfishes, and both chambers continue beating following an atrioventricular ligature, albeit with the atrium outpacing the ventricle (Jensen, 1965; Wilson and Farrell, 2013).

MATERIALS AND METHODS

Animal husbandry

All experiments were carried out in accordance with animal care policies of the University of British Columbia, the Bamfield Marine Sciences Centre, and the Department of Fisheries and Oceans Canada. Pacific hagfish [*Eptatretus stoutii* (Lockington 1878)] were caught near Bamfield Marine Sciences Centre, Bamfield, BC, Canada, using baited traps. Hagfish (100±1 g; mean ± s.e.m.) were transported to the Department of Fisheries and Oceans Canada, West Vancouver Laboratory, BC, Canada, where they were housed in a 4000 l fibreglass tank supplied with flow-through seawater (10±1°C) and fed squid weekly. Hagfish were fasted a minimum of 48 h prior to any experimental treatment.

Anoxia exposure

Individual hagfish were placed in darkened 2.5 l chambers that were continuously flushed with aerated seawater (10±1°C) at a flow rate of 0.5 l min^{-1} that was maintained throughout the experiments. Hagfish were left undisturbed for 24 h to habituate to the chamber, during which time they readopted their typical curled posture, as observed in the holding aquarium (see Cox et al., 2010). Anoxia was achieved in the same manner as in Cox et al. (Cox et al., 2010) by supplying the chambers with N_2-saturated seawater from two gas-exchange columns placed in series. The transition period to anoxia lasted less than 1 h (water oxygen concentration was measured continuously with an OxyGuard Handy MkIII, Birkerød, Denmark; accuracy ±0.1 mg l^{-1}). During the transition to anoxia, hagfish became slightly agitated before assuming a straightened position, as previously reported (Cox et al., 2010). Hagfish were maintained in flow-through anoxic seawater for 24 h, before quickly (under 30 min) restoring normoxic conditions for up to 36 h. Hagfish were sampled at the end of the 24-h anoxic period (no normoxic recovery, termed 0 h group), 2 h into normoxic recovery and 36 h into normoxic recovery (2 h and 36 h groups, respectively) (N=10 for each group). Control animals (N=10) were sampled after 84 h in the chamber in normoxic water. At each sample time, hagfish were rapidly removed from their chamber and killed by decapitation, and the branchial heart was dissected, freeing the atrium (7.7±1.2 mg) and ventricle (59.2±4.4 mg), prior to freeze-clamping each separately and storing them in liquid N_2. Tissues were stored at −80°C. The precise location of the hagfish sinoatrial node is unknown; therefore, it could not be reliably isolated.

RNA extraction

Total RNA was extracted from tissues using TRIzol reagent (Invitrogen, Carlsbad, CA, USA). Extractions followed a modified protocol outlined by Ellefsen et al. (Ellefsen et al., 2008). Briefly, each frozen tissue was weighed (atria 17.2±1.2 mg, ventricles 59.3±4.4 mg, means ± s.e.m.) and immersed in 60 µl TRIzol per milligram tissue. Then, 0.2 µl mg^{-1} tissue of an external RNA control gene (mw2060) was added and the tissue/TRIzol/mw2060 mixture was homogenized for 1 min using a T-25 Basic Homogenizer (IKA Works, Wilmington, NC, USA). The use of an external RNA control has been argued to be the most accurate method for the normalization of real-time RT-PCR data (Huggett et al., 2005). mw2060, a 2060-bp-long mRNA species from the cyanobacterium *Microcystis* cf. *wesenbergi* that shows no sequence homology to known vertebrate mRNA species, was recently developed as a more reliable method for the normalization of real-time RT-PCR data from tissues of anoxia-tolerant species than other commonly employed normalization techniques (Ellefsen et al., 2008). Additionally, the methodology allows for inter-tissue comparisons of target gene expression (Stecyk et al., 2012). Samples were then chilled on ice, vortexed, incubated at room temperature for 15 min and vortexed again. The maximum amount of tissue/TRIzol homogenate (up to 1 ml) was transferred to an Eppendorf tube before adding chloroform (20% of the volume of tissue/TRIzol homogenate). The mixture was incubated at room temperature for 3 min, vortexed, centrifuged at 10,000 ***g*** for 15 min at 4°C and placed on ice. A volume corresponding to 40% of the tissue/TRIzol homogenate of the upper aqueous phase was then transferred to a new Eppendorf tube before adding an equal amount of ice-chilled isopropanol. The mixture was vortexed, incubated at −20°C overnight, incubated at room temperature for 10 min and centrifuged at 11,500 ***g*** for 10 min at 4°C. The supernatant was then discarded and the pellet was washed twice with ice-chilled 75% ethanol. Each ethanol wash was followed by centrifugation at 11,500 ***g*** for 10 min at 4°C. After the final ethanol wash, the pellet was air dried and eluted in 30 µl of nuclease-free water (Ambion, Austin, TX, USA). The mixture was then

Table 1. Primers used for, and lengths of, partially cloned hagfish HCN genes

Gene		Primer for cloning	Amino acid length of partially cloned segment
HCN2a	F	TTCCTCATTGTGGAGAAGGG	291
HCN2b	R	GATTTCCCCGAAGTAGGAGC	367
HCN3a	F	GGGGAGCTGAGTGAGCCTCTCAAA	78
	R	TGTTGCCCTTGGTGAGGATGCTG	
HCN3bi	F	GCTGAGGTCTACAAGACGGC	283
HCN3bii	R	TAAAGGCGGCAGTAGGTGTC	304
HCN3c	F	CATGCCGCTGTTTGCCAAT	48
	R	CAAAGTAGGAGCCATCTGCCAGTTTAG	
HCN 4	F	TCCCAACTTTGTGACATCCA	65
	R	GGCAGTAGGTATCAGCTCGC	

HCN, hyperpolarization-activated cyclic nucleotide-gated channel; F, forward primer; R, reverse primer.

incubated at 65°C for 5 min to ensure the pellet was completely dissolved, and stored at −80°C.

Care was taken to avoid systematic errors introduced by sample processing during RNA extraction. All samples were handled without intermission and in a systematic, random order. Samples were processed in groups, wherein each group consisted of samples of a single tissue type and representing each of the treatment groups. The samples within each group were processed at random. Similar procedures were also employed for cDNA synthesis.

cDNA synthesis

The concentration of total RNA in every sample was determined using a NanoDrop ND-1000 UV-Vis Spectrophotometer (NanoDrop Technologies, Rockland, DE, USA). One microgram of total RNA from each sample was then treated with DNase I (DNA-free; Invitrogen) and subsequently reverse transcribed using Random Hexamers (50 ng μl^{-1}) and Superscript III (both from Invitrogen) in reaction volumes of 20 µl and in accordance with the manufacturer's protocol. cDNA solutions were diluted 1:30 with nuclease-free water and stored at −20°C. Duplicate cDNA syntheses were performed on RNA samples when possible.

Cloning of HCN genes

The HCN isoforms were partially cloned using PCR primers designed to recognize gene regions conserved among vertebrate species. The regions were located using GeneDoc (version 2.6.0.2, http://www.nrbsc.org/gfx/genedoc/) and ClustalX (version 1.81), while primers were designed using Primer3 (Nicholas et al., 1997; Thompson et al., 1997; Rozen and Skaletsky, 2000). Primers used for cloning are listed in Table 1.

PCR was performed on a mixture of 1:30 diluted cDNA from atrial and ventricular tissues and all treatment groups using Platinum *Taq* DNA Polymerase (Invitrogen; 94°C for 10 min, 94°C for 30 s, 48°C for 1 min, 72°C for 1 min, repeat steps two to four 44 times, 72°C for 10 min, hold 4°C). Resulting dsDNA fragments were ligated into the pGEM-T Easy Vector System I (Promega, Madison, WI, USA). Ligation reactions were transformed into $CaCl_2$-competent cells (TOP10 F′; Invitrogen) and positive colonies were checked for inserts of a correct size *via* agarose gel electrophoresis. PCR products from up to eight colonies were sequenced using T7 primers (ABI-lab, University of Oslo, Oslo, Norway). All procedures were carried out according to the manufacturer's protocol.

Analysis of partially cloned HCN genes

The partial sequences of cardiac HCN for hagfish were compared with known vertebrate HCN genes using ClustalX and NCBI BLAST (Altschul et al., 1990; Thompson et al., 1997). A phylogeny was created by running a neighbour-joining phylogenetic analysis with the translated amino acid products from the hagfish HCN isoforms, plus those of vertebrate species downloaded from Ensembl and GenBank. The closely related human ether-à-go-go-related gene (hERG) and *Drosophila* cyclic-nucleotide-gated gene (dCNG) were added to the sequence alignment as outgroups. A 37 amino acid segment was used because all partially cloned isoform protein segments overlapped in this area. One thousand bootstrap replications were conducted on the amino acid sequences and a consensus tree was produced. The phylogeny was completed using the Seqboot, Protdist, Neighbor, Consense and Drawgram programs of PHYLIP 3.65 (http://evolution.genetics.washington.edu/phylip.html), and viewed using TreeView 1.6.6 (http://taxonomy.zoology.gla.ac.uk/rod/treeview.html) and formatted using Adobe Illustrator (Page, 1996).

Real-time RT-PCR primer design and protocol

All real-time RT-PCR primer pairs were designed using Primer3. The small differences between the paralogs of HCN2 and HCN3b prevented distinctions between paralogs using the tested primers; therefore, both paralogs of HCN3b and HCN2 are compared collectively as HCN3b and HCN2, respectively. Forward and reverse primers were targeted to either side of an exon–exon overlap as a further precaution against amplifying genomic DNA (i.e. in addition to the extraction of total RNA and DNase treatment). Amplification of the desired cDNA species by the primer pairs was verified by melting curve analyses (Lightcycler 480 software, Roche Diagnostics, Basel, Switzerland) and cloning and sequencing of all primer pair products (performed as described above for the cloning of HCN genes). Real-time RT-PCR primer sequences are summarized in Table 2. To find primers that worked well with the real-time RT-PCR protocol (primer concentration of 1 mmol l^{-1} and

Table 2. Primers used for real-time RT-PCR

Gene		Primer for cloning
HCN2	F	GCATCCTGGGCGAGCTGAAC
	R	CCCGGCTGGAAGACCTCGAACTT
HCN3a	F	GGGGAGCTGAGTGAGCCTCTCAAA
	R	TGTTGCCCTTGGTGAGGATGCTG
HCN3b	F	CGTGCTATGCCATGTTCATC
	R	CCCCAAGAATGCTATCCTCA
HCN3c	F	CATGCCGCTGTTTGCCAAT
	R	CAAAGTAGGAGCCATCTGCCAGTTTAG
HCN 4	F	AGGGCACCATTGGCAAGAAA
	R	CAAAGTAGGAGCCATCTGCCAGTTAG

HCN, hyperpolarization-activated cyclic nucleotide-gated channel; F, forward primer; R, reverse primer.

annealing temperature of 60°C), a minimum of four primer pairs were tested for each gene. As an alternative to primer concentration/annealing temperature optimization, primer pairs that displayed distinct melting curves, the highest efficiency (calculated as described below for RT-PCR analyses) and the lowest C_q (quantification cycle) values were chosen. All procedures followed manufacturer's protocols.

Real-time RT-PCR for HCN isoforms 2, 3a, 3b and 3c were performed using Lightcycler 480. All real-time RT-PCR reactions were performed with a reaction volume of 10 µl that contained 5 µl of Lightcycler 480 SYBR Green I Master (Roche Diagnostics), 3 µl of 1:15 diluted cDNA as the template, 1 µl of 5 mmol l^{-1} gene-specific forward primer and 1 µl of 5 mmol l^{-1} gene-specific reverse primer (i.e. a final primer concentration of 1 mmol l^{-1}). The real-time RT-PCR program was: 95°C for 10 min, 95°C for 10 s and 60°C for 10 s, 72°C for 13 s, repeating steps two to four 42 times. Two real-time RT-PCR reactions were performed on each gene for each cDNA synthesis. The replicates were conducted on different

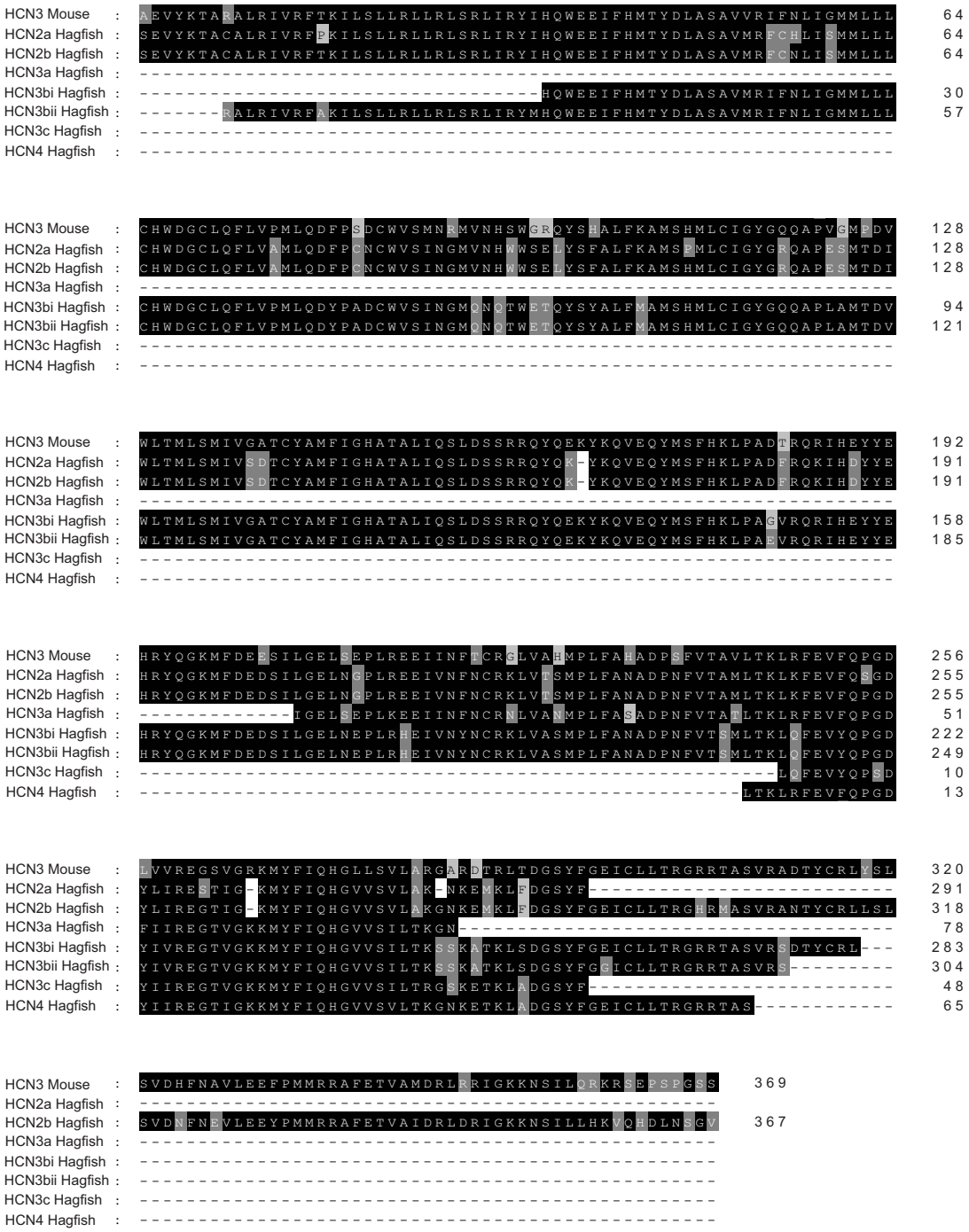

Fig. 1. Amino acid sequence comparison of partially cloned hagfish hyperpolarization-activated cyclic nucleotide-gated channel (HCN) isoforms. The segment of mouse HCN3 that aligns with hagfish sequences is also shown to highlight the large degree of sequence identity between the two species. Shading indicates four levels of sequence conservation, with darker shading corresponding to higher conservation. Genes were aligned using ClustalX, compared using GeneDoc and edited using Adobe Illustrator CS5.

plates and days. As a result, four real-time RT-PCR reactions were performed on each gene for each RNA sample.

For HCN4, real-time RT-PCR was conducted using an ABI Prism 7000 Sequence Detection System (Applied Biosystems, Foster City, CA, USA). Each real-time RT-PCR reaction contained 10 µl SYBR Green Master Mix (Applied Biosystems), 4 µl of 1:15 diluted cDNA as the template, 0.8 µl of 5 mmol l^{-1} gene-specific forward primer and 0.8 µl of 5 mmol l^{-1} gene-specific reverse primer and 4.4 µl of double-processed tissue-culture water (Sigma-Aldrich, Ayrshire, UK), bringing the total reaction volume to 20 µl. The real-time RT-PCR program was: 50°C for 2 min, 95°C for 10 min, 40 cycles of 95°C for 15 s and 60°C for 1 min. Following the real-time RT-PCR, a melt curve analysis was performed. As for the other isoforms, two real-time RT-PCR reactions were performed on each cDNA synthesis, resulting in four real-time RT-PCR reactions for each mRNA sample.

Real-time RT-PCR analysis

For HCN2, HCN3a, HCN3b and HCN3c, C_q values were obtained for each reaction using the Lightcycler 480 software and were defined according to the second derivative maximum (Luu-The et al., 2005). Priming efficiencies were calculated for each real-time RT-PCR reaction using LinRegPCR software (Ruijter et al., 2009). For HCN4, each plate was run with a standard dilution of a mixture of randomly chosen cDNA samples from atrial and ventricular tissues. The primer efficiencies were then determined for each plate from the slope of the standard curve using Applied Biosystems 7000 System Sequence Detection Software 1.2.3. This software was also used to obtain the C_q values for each reaction.

Average priming efficiencies ($\bar{E}$) were used for the final calculations, which were calculated separately for each tissue and primer pair from all real-time RT-PCR reactions (Čikoš et al., 2007). Then, to normalize HCN isoform gene expression to the expression of the external RNA control mw2060, $\bar{E}^{Cq}$ was calculated for every reaction, as well as the ratio (R1) between $\bar{E}_{mw2060}{}^{Cq}$ and $\bar{E}_{Tar}{}^{Cq}$ (where Tar is the target gene, E is priming efficiency and C_q is the quantification cycle). To compare the expression of each HCN isoform among the different treatments, R1 was referenced to the mean expression of the control, normoxic samples.

Calculations and statistical analyses

Results are expressed as means ± s.e.m. Statistical analyses were performed using SigmaPlot for Windows 11.0 (Systat Software, Chicago, IL, USA). Differences in HCN isoform expression within a tissue were assessed using a one-way ANOVA followed by a Tukey's *post hoc* test. A two-way ANOVA, followed by a Tukey's *post hoc* test, was used to determine statistically significant effects of anoxia and recovery on the expression of HCN gene isoforms. Differences in atrial and ventricular HCN isoform expression among each sampling time were assessed using a Student's *t*-test. Significance was accepted at $P<0.05$.

RESULTS

Phylogenetics

A total of six isoforms of HCN mRNA were found in hagfish cardiac tissue, with all six isoforms being represented at varying levels in both atrial and ventricular chambers and one isoform existing with two paralogs, for a total of seven partially cloned genes. The amino acid sequences aligned with mouse HCN3 are shown in Fig. 1 with the lengths of the partially cloned sequences shown in Table 1. Two isoforms of a hagfish representative of vertebrate HCN2, termed HCN2a and HCN2b, differed by five amino acid substitutions (P-

Fig. 2. Bootstrapped neighbour-joining phylogeny of hyperpolarization-activated cyclic nucleotide-gated channel (HCN) genes including hagfish HCN isoforms. Hagfish genes were partially cloned and sequenced from hagfish hearts. *Drosophila*, *Ciona* and vertebrate sequences were downloaded from GenBank and Ensembl. Sequences were aligned in ClustalX, edited and translated to amino acids in GeneDoc, and the phylogeny was compiled using Phylip-3.69 and edited using Adobe Illustrator CS5. The tree was run with 1000 bootstrap datasets, the low bootstrap values likely a consequence of both the short 37-amino-acid sequence used and a high sequence identity, as seen in Jackson et al. (Jackson et al., 2007). CNG, cyclic nucleotide gated channel; ERG, Ether-à-go-go-related gene. Nomenclature used by Jackson et al. (Jackson et al., 2007) is used with chicken abbreviated to hen for clarity. Scale bar represents 1% residue substitutions per site.

T at 16, H-N at 56, P-H at 111, S-P at 253, S-G at 261) and one deletion of a G at location 280 in HCN2a. Three isoforms of HCN3 were found, HCN3a, HCN3b and HCN3c, with HCN3b existing as two paralogs. These two paralogs, termed HCN3bi and HCN3bii, differed by two substitutions (G-E) at amino acid locations 148 and 262. One hagfish representative of HCN4 was also found.

Neighbour-joining phylogenetic analysis (Fig. 2) was conducted on a 37 amino acid sequence from the CNBD of multiple vertebrate and urochordate HCN genes where six of the seven hagfish sequences overlapped, as shown in Fig. 3 (HCN3bi and HCN3bii paralogs are included as HCN3b on the tree because the G-E substitutions of HCN3bi and HCN3bii occurred outside of this segment).

To summarise the phylogenetic tree, HCN3b and HCN3c cluster together and, along with HCN3a, form a cluster with the HCN3 of teleosts. The HCN3 of mammals cluster together on the other side of the outgroup, which contains both the HCN-related human ERG and *Drosophila* CNG proteins, as well as the *Ciona* HCN isoforms. The HCN4 isoforms, including the hagfish sequence, all cluster together apart from the pufferfish HCN4a isoforms. The hagfish HCN2 sequences cluster with the mammalian HCN2 and pufferfish HCN2b isoforms, while the other teleost HCN2 sequences cluster in a second group either side of the HCN1 cluster. The splitting of HCN isoforms in the tree may be a consequence of using short sequences for the analysis. Despite the lack of a hagfish HCN1 sequence in the phylogeny, it is noted that the two teleost HCN1 isoforms cluster as a separate branch of the HCN1 cluster.

HCN gene expression

Of the five measured hagfish HCN isoforms, HCN3a had the highest expression in both the atrium and ventricle in normoxia. HCN3a was expressed over 17 times more than HCN4 in the atrium and 25 times more than HCN4 in the ventricle (Fig. 4). Expression of the other isoforms followed the order of HCN4, HCN3b, HCN2 and HCN3c for both the atrium and the ventricle. Because of the similarity of the two HCN2 and HCN3b mRNA segments, it was not possible to distinguish between them using the real-time RT-PCR primers, and both segments would have been duplicated together by their respective primers.

Effects of anoxia on HCN gene expression

The effects of 24 h of anoxia and subsequent recovery on HCN isoform gene expression are shown in Fig. 5. In the atrium, the only statistically significant change was an increase in HCN3a at 2 h of normoxic recovery from anoxia, which returned to control expression levels by 36 h of recovery. In contrast, anoxia induced a significant

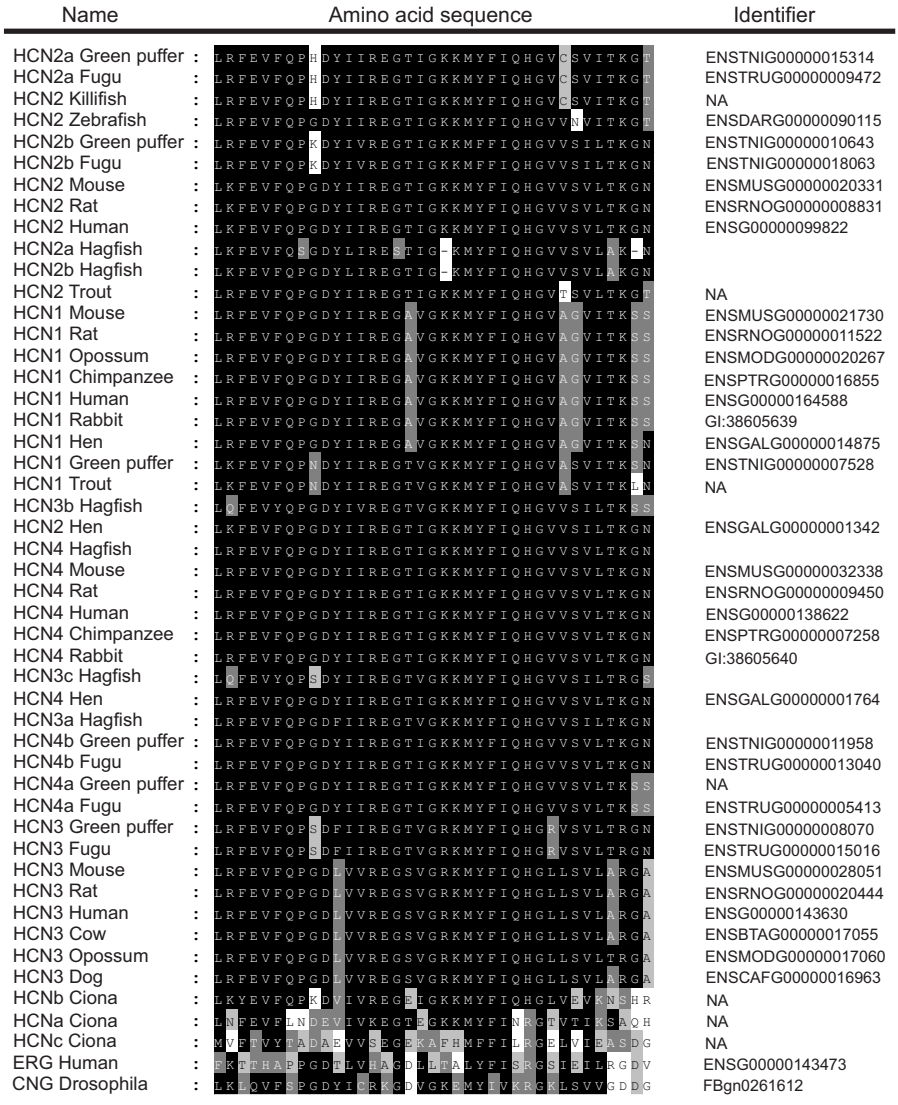

Fig. 3. Alignment of the overlapping, 37-amino-acid-long sequences from *Ciona*, hagfish and vertebrate hyperpolarization-activated cyclic nucleotide-gated channel (HCN) cyclic-nucleotide binding domain utilized in the phylogenetic analysis. Shading indicates four levels of sequence conservation, with darker shading corresponding to higher conservation. Genes were aligned using ClustalX, compared using GeneDoc and edited using Adobe Illustrator CS5. CNG, cyclic nucleotide gated channel; ERG, Ether-à-go-go-related gene. Hen=Chicken.

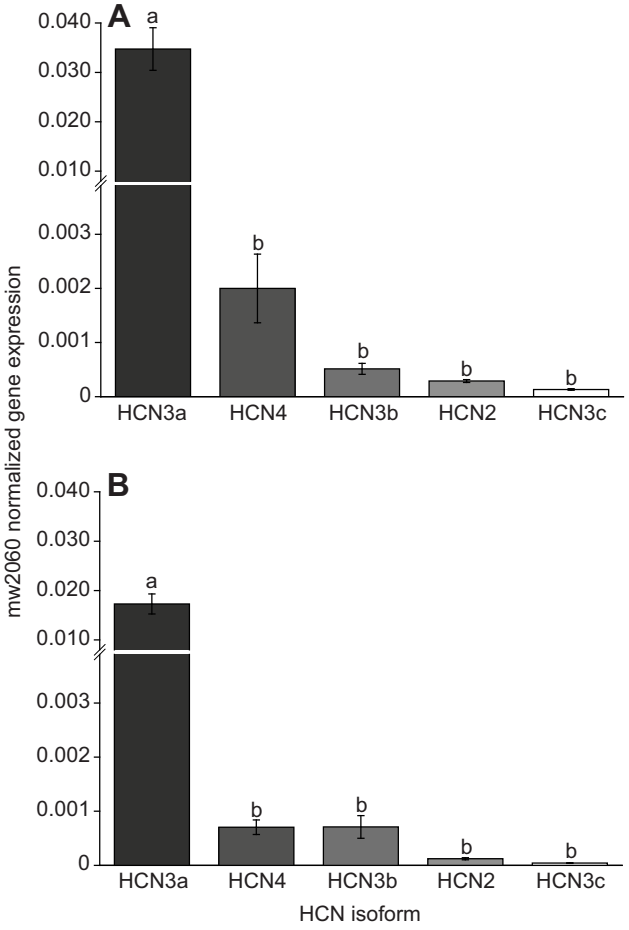

Fig. 4. A comparison of hyperpolarization-activated cyclic nucleotide-gated channel (HCN) gene isoform expression in hagfish atrium (A) and ventricle (B) under normoxic control conditions. Gene expression was measured by real-time RT-PCR and normalized to mw2060 control gene expression. Note the change in scale on the *y*-axis following the break. Dissimilar letters denote significant differences between gene expression (one-way ANOVA, $P<0.05$). $N=10$. Error bars show ±s.e.m.

decrease of HCN3a expression in the ventricle, which again progressively recovered back to the control level within the 36 h recovery period. The trends in HCN3b, HCN3c and HCN2 expression during anoxia, while not reaching statistical significance (Fig. 5), did return to the control values with normoxic recovery. Expressing HCN gene expression in the atrium and ventricle as ratio further illustrates the clear differences in the responses of the two chambers to anoxia (Table 3). For example, the ratio of atrial to ventricular HCN3b expression increased from <1 to 7 following 24 h of anoxia before returning back to <1 following 2 h of normoxic recovery.

DISCUSSION

The present study documents for the first time HCN expression in a representative of the basal chordates and elucidates differential changes in HCN expression in the atrium and ventricle of anoxic hagfish. Specifically, we: (1) described six isoforms of HCN from seven partial HCN amino acid sequences in the cardiac tissues of Pacific hagfish, (2) performed a phylogenetic analysis on six of these sequences, (3) made a quantitative comparison of the mRNA expression of five HCN isoforms for the atrium and ventricle and (4) discovered changes in HCN isoform expression in response to chronic anoxia that were reversed following normoxic recovery.

Six HCN isoforms were identified – HCN2a, HCN2b, HCN3a, HCN3b, HCN3c and HCN4 – a finding that differs from that in the adult mammalian heart, where four isoforms, HCN1–4, are expressed. Contrary to HCN4 dominance in mammalian pacemaker tissue (Shi et al., 1999; Marionneau et al., 2005), HCN3a was the dominantly expressed isoform in the hagfish atrium and ventricle. In addition, hagfish cardiac HCN3b existed as two paralogs, designated here as HCN3bi and HCN3bii. These findings have important implications for the phylogenetic appearance of pacemaker channels in the chordate lineage, as summarised in Fig. 6. Moreover, given what is known of the biophysical properties of the mammalian HCN isoforms, and assuming that mRNA expression reflects protein presence, the findings lend new but preliminary insights into the electrophysiological properties of the hagfish heart and possibly how heart rate is modulated during and following prolonged anoxia.

Based on the neighbour-joining phylogenetic analysis, the vertebrate HCN2, HCN3 and HCN4 isoforms had already appeared in cardiac tissues of the chordate lineage prior to the hagfish/gnathostome divergence. This conclusion is in accordance with previous work that compared HCN of *Ciona* with that of vertebrates, including more modern teleost species (Jackson et al., 2007). Jackson et al. proposed that HCN3 is ancestral, followed by the appearance of HCN4 and then HCN2 (Jackson et al., 2007). As shown here, all HCN3 isoforms cluster together and therefore appear ancestral. The two isoforms of HCN2 (2a and 2b) cluster together with the mammalian and avian forms of HCN2. Clearly, limitations do exist when using partial genes to create a phylogeny. Potentially, minor mutations of the CNBD during the long period between the appearance of hagfish and vertebrates may make ancestral genes appear more derived, something that will not be revealed with partial cloning and sequencing. However, a more robust phylogeny will require full hagfish HCN sequences. Nevertheless, the CNBD has been highly conserved throughout evolution (Jackson et al., 2007), likely because of its important regulatory function. Indeed, changing a single amino acid in this region is known to appreciably alter the effect of cAMP binding to the CNBD (Tibbs et al., 1998). Also, HCN2 and HCN4 are strongly gated by cAMP, whereas HCN1 is not (Wang et al., 2001). Moreover, because three lineage-specific HCN isoforms have been reported previously in urochordates (Jackson et al., 2007), it was previously hypothesised that, prior to the divergence of the deuterostomes, duplication of the ancestral HCN gene gave the sea urchin two HCN isoforms and, because of a further duplication, three HCN isoforms were found in the urochordates (Gauss et al., 1998; Galindo et al., 2005; Jackson et al., 2007). A further possibility is that the sea urchin also had three HCN isoforms, but subsequently lost one. It has been suggested that HCNa, HCNb and HCNc emerged early in *Ciona*, before *C. intestinalis* and *C. savignyi* had diverged; therefore, these three HCN isoforms may have been present in the urochordate ancestor (Jackson et al., 2007). Because the three hagfish HCN3 isoforms do not align with the *Ciona* isoforms, it is unlikely that the hagfish HCN3a, HCN3b and HCN3c isoforms represent an ancestral condition prior to the urochordate/chordate divergence, and more likely represent HCN3 duplication events following the hagfish/vertebrate split.

What is apparent from the available information is that lineage-specific HCN gene duplications are relatively regular evolutionary events, being previously identified in the urochordates and some teleost fishes (Gauss et al., 1998; Galindo et al., 2005; Jackson et al., 2007), and now in hagfishes. Having many isoforms of these genes could provide flexibility and fine-tuning of pacemaker

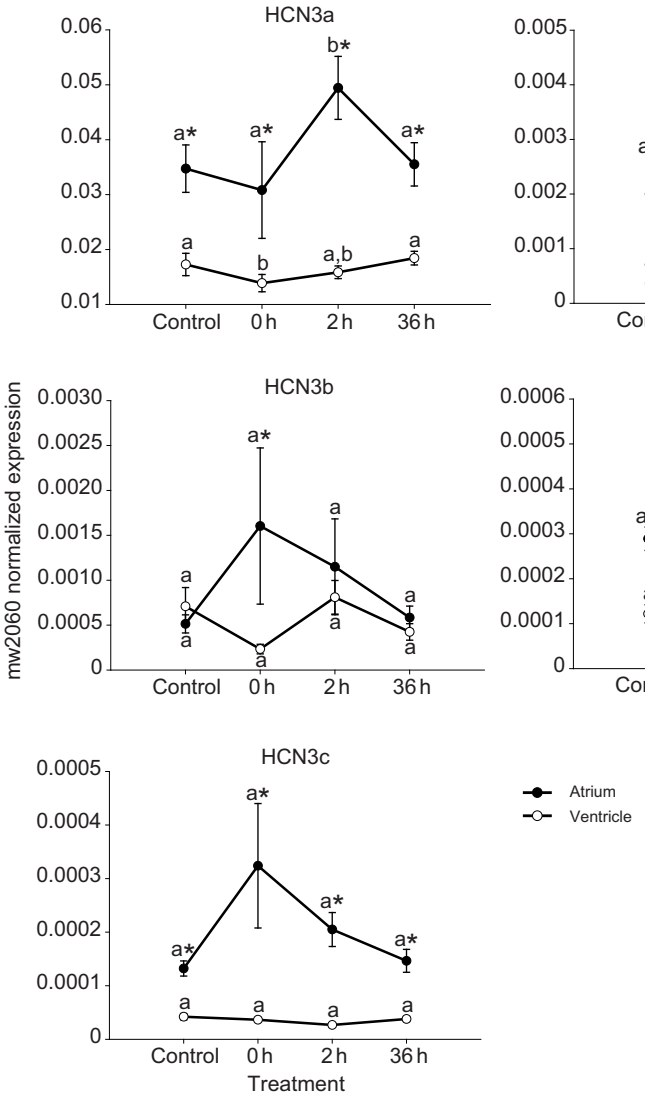

Fig. 5. Effect of 24 h anoxia (0 h) and normoxic recovery following 24 h anoxia (2 h and 36 h) on hyperpolarization-activated cyclic nucleotide-gated channel (HCN) isoform gene expression in atrium and ventricle of hagfish hearts. Gene expression was measured by real-time RT-PCR and normalized to mw2060 control gene expression. Dissimilar letters denote significant differences within a tissue among treatment times (two-way ANOVA, $P<0.05$) and an asterisk denotes significantly higher gene expression in the atrium compared with the ventricle at a specific treatment time (*t*-test, $P<0.05$). $N=10$ for all groups except $N=9$ for 0 h ventricles. Error bars show ±s.e.m.

activity, perhaps providing an evolutionary advantage, which we speculate on below.

Many primers were used without success to target conserved regions of the vertebrate HCN1 isoform in the hagfish heart. We propose three possible explanations for the absence of HCN1 in the hagfish heart. First, HCN1 is commonly associated with central neural tissue in addition to the heart (Franz et al., 2000; Nolan et al., 2003). Therefore, HCN1 expression in hagfish may be limited to non-cardiac tissues. Another explanation could be related to a very low expression of HCN1 that was below the detection level. Finally, HCN1 may not have appeared in the vertebrate lineage until after the hagfish/vertebrate split. Failure to find HCN1 in hagfish would suggest that duplication of the ancestral HCN2-like gene likely produced HCN1 following the hagfish/vertebrate divergence. Indeed, in another phylogenetic study, HCN1 was suggested as the most recent HCN gene, although the exact timing of its appearance is unknown (Jackson et al., 2007). Data on HCN expression in elasmobranchs and basal teleosts would be particularly informative in this regard. All the same, conclusive knowledge on the exact number and type of HCN isoforms will not be possible until the entire hagfish genome has been sequenced and searched.

Table 3. Ratio of atrial to ventricular HCN gene expression in hagfish hearts during normoxia (control), at the end of (0 h) and during recovery (2 h and 36 h) from a 24-h anoxic period

	Treatment			
Gene	Control	0 h	2 h	36 h
HCN2	2	3	2	2
HCN3a	2	2	3	2
HCN3b	<1	7	<1	<1
HCN3c	3	9	8	4
HCN4	3	<1	<1	3

Values are rounded to the nearest whole number.
HCN, hyperpolarization-activated cyclic nucleotide-gated channel.

In mammalian studies, HCN4 is by far the most dominant HCN isoform in the heart, with expression in the sinoatrial node dwarfing that of other HCN channels (Shi et al., 1999; Marionneau et al., 2005). Contrary to this, we discovered that in hagfish, HCN3a mRNA expression in both the atrium and ventricle dominates HCN4 mRNA expression by at least an order of magnitude (Fig. 4). In this regard, the hagfish heart bears some resemblance to mammalian embryonic stem cells, where, in early stage mouse embryonic stem cells, the dominant HCN isoform is HCN3 (Qu et al., 2008). As mouse development progresses, expression of HCN3 decreases and

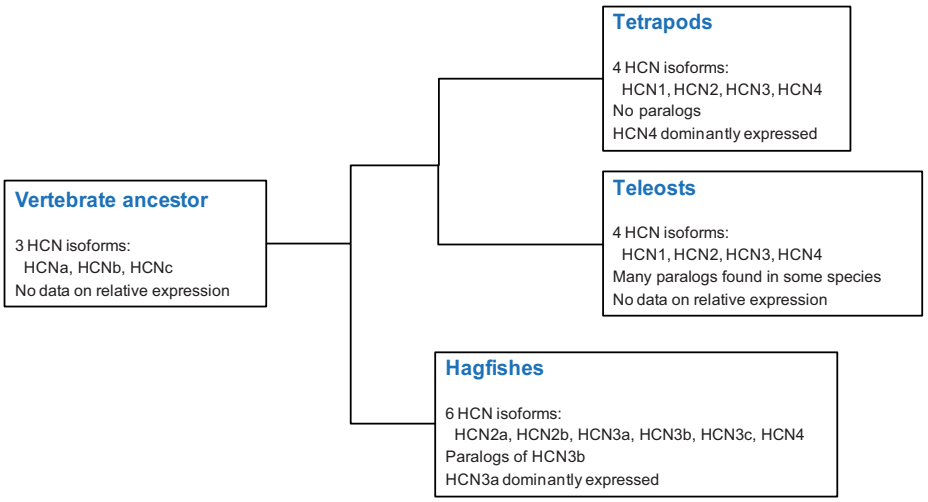

Fig. 6. Summary of phylogenetics and hyperpolarization-activated cyclic nucleotide-gated channel (HCN) isoform expression in chordates, showing the known presence of HCN isoforms, paralogs resulting from duplications of an HCN isoform and dominantly expressed HCN isoforms. Prior to the angnathan/gnathostome split, at least three of the four vertebrate HCN isoforms had appeared. Since this split, likely through gene-specific duplications and mutations, at least five isoforms plus two paralogs emerged in the hagfishes. The emergence of paralogs also took place in the teleost lineage. Following the emergence of the gnathostomes, a reliance on HCN4 as the dominantly expressed HCN isoform occurred. When this happened is presently unknown because of the lack of HCN expression data from teleost fishes and ancestral tetrapods.

HCN4 becomes dominant in association with the onset of cardiac contractions (Qu et al., 2008; Schweizer et al., 2009). While we are not prescribing Lamarkian recapitulation of phylogeny, the similarity points to a functional role of variations in cardiac HCN isoform expression. Nevertheless, care must be taken when speculating on the physiological implications of differential HCN isoform expression in the hagfish because the electrophysiological properties of these new isoforms have yet to be examined. Therefore, the electrophysiological ramifications of the present results that are proposed below are based on the rich knowledge of mammalian HCN electrophysiology.

In lieu of electrophysiological evidence on the activation dynamics of the hagfish HCN isoforms, it is not possible to know exactly what the effect of HCN3 dominance over HCN4 might be on hagfish cardiac excitation–contraction coupling. However, Moosmang et al. (Moosmang et al., 2001) showed that HCN3 activates at a similar voltage to HCN4, but has activation kinetics more similar to the faster HCN2 isoform, allowing a larger current to flow at lower membrane potentials. Therefore, a large proportion of HCN3 may allow the hagfish heart to become easily activated and then allow the spread of excitation throughout the myocardium to occur rapidly. Indeed, evidence exists for the presence of pacemaker potentials throughout the hagfish myocardium, which may be a requirement to allow enough current to flow in order to activate contraction in a heart known to have a low diastolic membrane potential (Jensen, 1965).

A higher HCN mRNA expression in the hagfish atrium compared with the ventricle for all isoforms of HCN (apart from the similar expression of HCN3b) was to be expected for synchronous cardiac contraction, as it would cause the atrial pacemaker potential to be shorter than that of the ventricle. Indeed, HCN gene expression per unit mass in rabbit atria and especially the sinoatrial node are much higher than that in the ventricles (Shi et al., 1999; Moosmang et al., 2001; Marionneau et al., 2005). In turn, a larger sarcolemmal ion channel density allows a larger current to pass when the membrane channels are open (Mukherjee et al., 1998). Thus, a higher atrial HCN channel expression leads to a larger I_f and a faster depolarisation to the threshold potential between action potentials, which ensures that atrial contraction precedes ventricular contraction. Although expression of four out of five isoforms was roughly twice as high in the atrium compared with the ventricle, we have no information on sarcolemmal protein expression. However, it seems that relative excitation, and therefore synchrony of contraction, of hagfish cardiac chambers is controlled primarily by HCN3a channel density rather than upregulation and downregulation of specific isoforms in the chambers. Indeed, it is possible that regulation of HCN channel density throughout the myocardium may be a precursor of the cardiac conduction system seen in other vertebrate hearts.

We postulated, and our data support the idea, that alterations in HCN channel expression could play a role in controlling heart rate during prolonged anoxia and subsequent recovery. Consistent with the 50% decrease in heart rate during anoxia, an increased heart rate during the initial phase of recovery and the return of heart rate to the control normoxic rate after 36 h of recovery (Cox et al., 2010), we discovered significant changes in HCN mRNA expression with anoxia and recovery. Ventricular HCN3a expression decreased significantly, with the HCN3a:HCN4 expression ratio decreasing by over threefold, from 25:1 to 7:1 during anoxia and returning to 20:1 during normoxic recovery (Table 4). In contrast, the HCN3a:HCN4 expression ratio increased almost twofold in the atrium, from 17:1 to 26:1 during anoxia, and returned to 12:1 during normoxic recovery (Table 4). In mammals, HCN4 allows a smaller current to flow compared with HCN3; therefore, these findings may represent a decrease in hagfish ventricular excitability during prolonged anoxia. The immediate response to restoration of normoxic conditions for the hagfish heart is a quadrupling of the anoxia-induced heart rate after 2 h (Cox et al., 2010), which correlates with the increase in atrial HCN3a and a restored level of ventricular HCN3a. An increase in HCN3a would increase I_f, leading to an increased pacemaker potential, and therefore an increase in heart rate because the action potential upstroke threshold would be reached earlier. HCN3a expression returned to control levels by the end

Table 4. Ratio of HCN3a to HCN4 expression in hagfish atria and ventricles during normoxia (control), at the end of (0 h) and during recovery (2 h and 36 h) from a 24-h anoxic period

Treatment	Atria	Ventricles
Control	17	25
0 h	26	7
2 h	24	7
36 h	12	20

Values are rounded to the nearest whole number.
HCN, hyperpolarization-activated cyclic nucleotide-gated channel.

of the 36 h recovery period as did the ratio of HCN3a:HCN4 in both cardiac chambers. Therefore, it is possible that regulation of HCN3a may play a role, amongst others, in controlling heart rate during prolonged anoxia and subsequent recovery; however, these hypotheses need to be tested using protein expression studies.

The above discussion considered the HCN channel as the primary vertebrate cardiac pacemaker, yet a recent alternative hypothesis suggests that pacemaker activity involves a calcium clock (Rubenstein and Lipsius, 1989; Li et al., 1997; Hüser et al., 2000; Ju and Allen, 2000; Dobrzynski et al., 2007; Maltsev and Lakatta, 2008; Monfredi et al., 2013). In brief, this hypothesis proposes that spontaneous Ca^{2+} sparks released from the sarcoplasmic reticulum *via* ryanodine receptors interact with local sodium-calcium exchanger proteins to cause an overall inward depolarizing current. The Ca^{2+} is then pumped back into the sarcoplasmic reticulum, thus resetting the clock. The most recent synthesis of experimental evidence in support of the calcium clock hypothesis includes HCN as a part, albeit a minor one, of the inter-related cycling of ions in pacemaker tissue (Monfredi et al., 2013). That said, this model does recognize that future work is still needed to completely explain how HCN blockers such as ZD7288 exert their effect within the calcium clock paradigm. Moreover, future calcium clock studies will have to resolve why another HCN blocker, zatebradine, which slows pacemaker activity in rainbow trout hearts (Gamperl et al., 2011), almost completely abolished pacemaker activity in both atrial and ventricular chambers isolated from hagfish (Wilson and Farrell, 2013), and how recent work in mice has shown that an increase in heart rate during pregnancy is coupled with an increase in HCN2 expression (El Khoury et al., 2013).

In summary, we have provided novel insights into cardiac pacemaker expression and their evolution using real-time RT-PCR of partially cloned HCN mRNA expression in hagfish hearts under normoxic and anoxic conditions. Of the six isoforms, HCN3a dominated in atrium and ventricle. The presence of HCN2, HCN3 and HCN4 in the hagfish heart suggests their presence prior to the hagfish/vertebrate divergence and an importance in cardiac pacemaker activity at the time of the emergence of the chambered myogenic heart. HCNa and HCNb appeared as either hagfish-specific duplications or remnants of the forms previously identified in ancestral deuterostomes and urochodates. Our postulate that altered HCN expression is involved in the control of heart rate in the aneural hagfish heart was supported by several observations, including a decrease in the ventricular HCN3 expression during anoxia and an increase in atrial HCN3 expression shortly after return to normoxia. Functional studies on the activation and cAMP gating of each isoform, and their respective roles in cardiac pacing, will require electrophysiological study, which, when coupled with HCN protein expression studies, will provide even further insight into regulation of heart rate in the aneural hagfish heart.

LIST OF SYMBOLS AND ABBREVIATIONS

CNBD	cyclic nucleotide-binding domain
C_q	quantification cycle
dCNG	*Drosophila* cyclic-nucleotide-gated gene
E	priming efficiency
$\bar{E}$	mean priming efficiency
HCN	hyperpolarization-activated, cyclic nucleotide-gated channel
hERG	human ether-à-go-go-related gene
I_f	mixed K^+ and Na^{2+} (funny) current
I_{NCX}	sodium/calcium exchange current
RT-PCR	reverse transcriptase polymerase chain reaction
Tar	target gene

ACKNOWLEDGEMENTS

Gratitude is given to Dr P. Schulte and T. Healy at the University of British Columbia for expertise and lab space during HCN4 measurements.

AUTHOR CONTRIBUTIONS

C.M.W. contributed to experimental design, performed all experiments, analyzed the data and produced the first draft of the manuscript. J.A.W.S. contributed to experimental design, primer design, real-time PCR experiments and phylogenetics. C.S.C. contributed to primer design, real-time PCR experiments, phylogenetics and data analysis. G.E.N. contributed to experimental design, real-time PCR experiments and phylogenetics. A.P.F. conceived the investigation and contributed to experimental design and production of the first draft of the manuscript. All authors contributed to interpretation of the results and manuscript revision.

COMPETING INTERESTS

No competing interests declared.

FUNDING

The research program of A.P.F. is supported by a Canada Research Chair and a Discovery Grant from the Natural Sciences and Engineering Research Council of Canada. A University Graduate Fellowship was awarded to C.M.W. The research program of G.E.N. is supported by the Research Council of Norway.

REFERENCES

Altschul, S. F., Gish, W., Miller, W., Myers, E. W. and Lipman, D. J. (1990). Basic local alignment search tool. *J. Mol. Biol.* **215**, 403-410.

Augustinsson, K.-B., Fange, R., Johnels, A. and Östlund, E. (1956). Histological, physiological and biochemical studies on the heart of two cyclostomes, hagfish (Myxine) and lamprey (Lampetra). *J. Physiol.* **131**, 257-276.

Baker, K., Warren, K. S., Yellen, G. and Fishman, M. C. (1997). Defective 'pacemaker' current (I_h) in a zebrafish mutant with a slow heart rate. *Proc. Natl. Acad. Sci. USA* **94**, 4554-4559.

Biel, M., Schneider, A. and Wahl, C. (2002). Cardiac HCN channels: structure, function, and modulation. *Trends Cardiovasc. Med.* **12**, 206-212.

Brown, H. F. and DiFrancesco, D. (1980). Voltage-clamp investigations of membrane currents underlying pace-maker activity in rabbit sino-atrial node. *J. Physiol.* **308**, 331-351.

Brown, H. F., DiFrancesco, D. and Noble, S. J. (1979a). How does adrenaline accelerate the heart? *Nature* **280**, 235-236.

Brown, H. F., Difrancesco, D. and Noble, S. (1979b). Cardiac pacemaker oscillation and its modulation by autonomic transmitters. *J. Exp. Biol.* **81**, 175-204.

Čikoš, Š., Bukovská, A. and Koppel, J. (2007). Relative quantification of mRNA: comparison of methods currently used for real-time PCR data analysis. *BMC Mol. Biol.* **8**, 113.

Cox, G. K., Sandblom, E. and Farrell, A. P. (2010). Cardiac responses to anoxia in the Pacific hagfish, *Eptatretus stoutii*. *J. Exp. Biol.* **213**, 3692-3698.

DiFrancesco, D. (1985). The cardiac hyperpolarizing-activated current, I_f. Origins and developments. *Prog. Biophys. Mol. Biol.* **46**, 163-183.

DiFrancesco, D. (1993). Pacemaker mechanisms in cardiac tissue. *Annu. Rev. Physiol.* **55**, 455-472.

DiFrancesco, D. (2010). The role of the funny current in pacemaker activity. *Circ. Res.* **106**, 434-446.

DiFrancesco, D. and Ojeda, C. (1980). Properties of the current i_f in the sino-atrial node of the rabbit compared with those of the current i_{K_2}, in Purkinje fibres. *J. Physiol.* **308**, 353-367.

DiFrancesco, D. and Tortora, P. (1991). Direct activation of cardiac pacemaker channels by intracellular cyclic AMP. *Nature* **351**, 145-147.

Dobrzynski, H., Boyett, M. R. and Anderson, R. H. (2007). New insights into pacemaker activity: promoting understanding of sick sinus syndrome. *Circulation* **115**, 1921-1932.

Doerr, T., Denger, R. and Trautwein, W. (1989). Calcium currents in single SA nodal cells of the rabbit heart studied with action potential clamp. *Pflugers Arch.* **413**, 599-603.

Doyle, D. A., Morais Cabral, J., Pfuetzner, R. A., Kuo, A., Gulbis, J. M., Cohen, S. L., Chait, B. T. and MacKinnon, R. (1998). The structure of the potassium channel: molecular basis of K^+ conduction and selectivity. *Science* **280**, 69-77.

El Khoury, N., Mathieu, S., Marger, L., Ross, J., El Gebeily, G., Ethier, N. and Fiset, C. (2013). Upregulation of the hyperpolarization-activated current increases pacemaker activity of the sinoatrial node and heart rate during pregnancy in mice. *Circulation* **127**, 2009-2020.

Ellefsen, S., Stensløkken, K.-O., Sandvik, G. K., Kristensen, T. A. and Nilsson, G. E. (2008). Improved normalization of real-time reverse transcriptase polymerase chain reaction data using an external RNA control. *Anal. Biochem.* **376**, 83-93.

Farrell, A. P. (2007). Cardiovascular systems in primitive fishes. In *Fish Physiology Vol. 26. Primitive Fishes* (ed. D. J. McKenzie, A. P. Farrell and C. J. Brauner), pp. 53-120. London: Academic Press.

Franz, O., Liss, B., Neu, A. and Roeper, J. (2000). Single-cell mRNA expression of HCN1 correlates with a fast gating phenotype of hyperpolarization-activated cyclic nucleotide-gated ion channels (Ih) in central neurons. *Eur. J. Neurosci.* **12**, 2685-2693.

Galindo, B. E., Neill, A. T. and Vacquier, V. D. (2005). A new hyperpolarization-activated, cyclic nucleotide-gated channel from sea urchin sperm flagella. *Biochem. Biophys. Res. Commun.* **334**, 96-101.

Gamperl, A. K., Swafford, B. L. and Rodnick, K. J. (2011). Elevated temperature, per se, does not limit the ability of rainbow trout to increase stroke volume. *J. Therm. Biol.* **36**, 7-14.
Gauss, R., Seifert, R. and Kaupp, U. B. (1998). Molecular identification of a hyperpolarization-activated channel in sea urchin sperm. *Nature* **393**, 583-587.
Greene, C. W. (1902). Contributions to the physiology if the California hagfish, *Polistotrema stouti*. II. The absence of regulative nerves for the systemic heart. *Am. J. Physiol.* **6**, 318-324.
Hirsch, E. F., Jellinek, M. and Cooper, T. (1964). Innervation of the systemic heart of the California hagfish. *Circ. Res.* **14**, 212-217.
Huggett, J., Dheda, K., Bustin, S. and Zumla, A. (2005). Real-time RT-PCR normalisation; strategies and considerations. *Genes Immun.* **6**, 279-284.
Hüser, J., Blatter, L. A. and Lipsius, S. L. (2000). Intracellular Ca^{2+} release contributes to automaticity in cat atrial pacemaker cells. *J. Physiol.* **524**, 415-422.
Ishii, T. M., Takano, M., Xie, L. H., Noma, A. and Ohmori, H. (1999). Molecular characterization of the hyperpolarization-activated cation channel in rabbit heart sinoatrial node. *J. Biol. Chem.* **274**, 12835-12839.
Jackson, H. A., Marshall, C. R. and Accili, E. A. (2007). Evolution and structural diversification of hyperpolarization-activated cyclic nucleotide-gated channel genes. *Physiol. Genomics* **29**, 231-245.
Jensen, D. (1961). Cardioregulation in an aneural heart. *Comp. Biochem. Physiol.* **2**, 181-201.
Jensen, D. (1965). The aneural heart of the hagfish. *Ann. N. Y. Acad. Sci.* **127**, 443-458.
Jiang, Y., Lee, A., Chen, J., Ruta, V., Cadene, M., Chait, B. T. and MacKinnon, R. (2003). X-ray structure of a voltage-dependent K+ channel. *Nature* **423**, 33-41.
Ju, Y. K. and Allen, D. G. (2000). The distribution of calcium in toad cardiac pacemaker cells during spontaneous firing. *Pflugers Arch.* **441**, 219-227.
Li, J., Qu, J. and Nathan, R. D. (1997). Ionic basis of ryanodine's negative chronotropic effect on pacemaker cells isolated from the sinoatrial node. *Am. J. Physiol. Heart. Circ. Physiol.* **275**, H2481-H2489.
Luu-The, V., Paquet, N., Calvo, E. and Cumps, J. (2005). Improved real-time RT-PCR method for high-throughput measurements using second derivative calculation and double correction. *Biotechniques* **38**, 287-293.
Maltsev, V. A. and Lakatta, E. G. (2008). Dynamic interactions of an intracellular Ca^{2+} clock and membrane ion channel clock underlie robust initiation and regulation of cardiac pacemaker function. *Cardiovasc. Res.* **77**, 274-284.
Marionneau, C., Couette, B., Liu, J., Li, H., Mangoni, M. E., Nargeot, J., Lei, M., Escande, D. and Demolombe, S. (2005). Specific pattern of ionic channel gene expression associated with pacemaker activity in the mouse heart. *J. Physiol.* **562**, 223-234.
Monfredi, O., Maltsev, V. A. and Lakatta, E. G. (2013). Modern concepts concerning the origin of the heartbeat. *Physiology* **28**, 74-92.
Moosmang, S., Stieber, J., Zong, X., Biel, M., Hofmann, F. and Ludwig, A. (2001). Cellular expression and functional characterization of four hyperpolarization-activated pacemaker channels in cardiac and neuronal tissues. *Eur. J. Biochem.* **268**, 1646-1652.
Mukherjee, R., Hewett, K. W., Walker, J. D., Basler, C. G. and Spinale, F. G. (1998). Changes in L-type calcium channel abundance and function during the transition to pacing-induced congestive heart failure. *Cardiovasc. Res.* **37**, 432-444.
Nicholas, K. B., Nicholas, H. B. J. and Deerfield, D. W. (1997). GeneDoc: analysis and visualization of genetic variation. *EMBnet News* **4**, 1-4.
Nolan, M. F., Malleret, G., Lee, K. H., Gibbs, E., Dudman, J. T., Santoro, B., Yin, D., Thompson, R. F., Siegelbaum, S. A., Kandel, E. R. et al. (2003). The hyperpolarization-activated HCN1 channel is important for motor learning and neuronal integration by cerebellar Purkinje cells. *Cell* **115**, 551-564.
Ota, K. G. and Kuratani, S. (2007). Cyclostome embryology and early evolutionary history of vertebrates. *Integr. Comp. Biol.* **47**, 329-337.
Page, R. D. (1996). TreeView: an application to display phylogenetic trees on personal computers. *Comput. Appl. Biosci.* **12**, 357-358.
Qu, J., Altomare, C., Bucchi, A., DiFrancesco, D. and Robinson, R. B. (2002). Functional comparison of HCN isoforms expressed in ventricular and HEK 293 cells. *Pflugers Arch.* **444**, 597-601.
Qu, Y., Whitaker, G. M., Hove-Madsen, L., Tibbits, G. F. and Accili, E. A. (2008). Hyperpolarization-activated cyclic nucleotide-modulated 'HCN' channels confer regular and faster rhythmicity to beating mouse embryonic stem cells. *J. Physiol.* **586**, 701-716.
Rozen, S. and Skaletsky, H. (2000). Primer3 on the WWW for general users and for biologist programmers. *Methods Mol. Biol.* **132**, 365-386.
Rubenstein, D. S. and Lipsius, S. L. (1989). Mechanisms of automaticity in subsidiary pacemakers from cat right atrium. *Circ. Res.* **64**, 648-657.
Ruijter, J. M., Ramakers, C., Hoogaars, W. M., Karlen, Y., Bakker, O., van den Hoff, M. J. B. and Moorman, A. F. M. (2009). Amplification efficiency: linking baseline and bias in the analysis of quantitative PCR data. *Nucleic Acids Res.* **37**, e45.
Schweizer, P. A., Yampolsky, P., Malik, R., Thomas, D., Zehelein, J., Katus, H. A. and Koenen, M. (2009). Transcription profiling of HCN-channel isotypes throughout mouse cardiac development. *Basic Res. Cardiol.* **104**, 621-629.
Shi, W., Wymore, R., Yu, H., Wu, J., Wymore, R. T., Pan, Z., Robinson, R. B., Dixon, J. E., McKinnon, D. and Cohen, I. S. (1999). Distribution and prevalence of hyperpolarization-activated cation channel (HCN) mRNA expression in cardiac tissues. *Circ. Res.* **85**, e1-e6.
Stecyk, J. A. W., Couturier, C. S., Fagernes, C. E., Ellefsen, S. and Nilsson, G. E. (2012). Quantification of heat shock protein mRNA expression in warm and cold anoxic turtles (*Trachemys scripta*) using an external RNA control for normalization. *Comp. Biochem. Physiol.* **7D**, 59-72.
Thompson, J. D., Gibson, T. J., Plewniak, F., Jeanmougin, F. and Higgins, D. G. (1997). The CLUSTAL_X windows interface: flexible strategies for multiple sequence alignment aided by quality analysis tools. *Nucleic Acids Res.* **25**, 4876-4882.
Tibbs, G. R., Liu, D. T., Leypold, B. G. and Siegelbaum, S. A. (1998). A state-independent interaction between ligand and a conserved arginine residue in cyclic nucleotide-gated channels reveals a functional polarity of the cyclic nucleotide binding site. *J. Biol. Chem.* **273**, 4497-4505.
Wainger, B. J., DeGennaro, M., Santoro, B., Siegelbaum, S. A. and Tibbs, G. R. (2001). Molecular mechanism of cAMP modulation of HCN pacemaker channels. *Nature* **411**, 805-810.
Wang, J., Chen, S. and Siegelbaum, S. A. (2001). Regulation of hyperpolarization-activated HCN channel gating and cAMP modulation due to interactions of COOH terminus and core transmembrane regions. *J. Gen. Physiol.* **118**, 237-250.
Wilson, C. M. and Farrell, A. P. (2013). Pharmacological characterization of the heartbeat in an extant vertebrate ancestor, the Pacific hagfish, *Eptatretus stoutii*. *Comp. Biochem. Physiol.* **164A**, 258-263.
Yanagihara, K. and Irisawa, H. (1980). Inward current activated during hyperpolarization in the rabbit sinoatrial node cell. *Pflugers Arch.* **385**, 11-19.